

Comparative Heat Flux Measurement of a Sharp Cone Between Three Hypersonic Test Facilities at LHD



Q. Wang, P. Lu, J. W. Li, S. Wu, J. P. Li, W. Zhao, and Z. L. Jiang

Abstract Comparative heat flux measurements for a sharp cone model were conducted by utilizing a high Reynolds number shock tunnel JF8A, a high-enthalpy shock tunnel JF10, and a large-scale shock tunnel JF12 at the Key Laboratory of High Temperature Gas Dynamics (LHD), Institute of Mechanics, Chinese Academy of Sciences, which were responsible for providing the nonequilibrium or perfect gas flows. Through the assessment of data accuracy and consistency between each facility, we aim to compare the heat transfer data of a sharp cone taken in them under a totally different kind of freestream conditions. A parameter, defined as the product of the Stanton number and the square root of the Reynolds number, was found to be more characteristic for the aerodynamic heating phenomena encountered in hypersonic flight under laminar flows. This parameter can almost eliminate the variability caused by the different flow conditions, and it should be a more preferable parameter for the reduction of the ground experimental data and the extrapolation to flight.

1 Introduction

Reliable prediction of heat transfer rates is a major issue for researchers and developers working within the current space program. For the high costs of flight tests, most aerodynamic heating experiments are still completed in the ground facilities, where shock tunnels show their advantages for the accommodation of

Q. Wang (✉) · J. W. Li · S. Wu · J. P. Li

State Key Laboratory of High Temperature Gas Dynamics, Institute of Mechanics, Chinese Academy of Sciences, Beijing, China

e-mail: wangqiu@imech.ac.cn

P. Lu · W. Zhao · Z. L. Jiang

State Key Laboratory of High Temperature Gas Dynamics, Institute of Mechanics, Chinese Academy of Sciences, Beijing, China

School of Engineering Science, University of Chinese Academy of Sciences, Beijing, China

relatively large-sized models and low operational costs. And the development of experimental technique has made it possible to realize hypersonic flows ranging from 2.5 to 45 MJ/kg, which corresponds to velocities from 2 to 10 km/s, respectively [1, 2]. However, no single ground test facility can fully simulate the many aspects of hypersonic flights; similarity parameters, such as Reynolds number and Mach number, are somewhat different from each other for different facilities due to their capability difference, which makes it difficult for the analysis, extrapolation, comparison, using of the experimental data [3]. Therefore, database or principles obtained from original models are necessary to be considered, which can provide guidance for comparison between different ground facilities or from ground to flight extrapolation. And cones are often the object of investigations for their relative simplicity of the flow fields and widespread use in missile designs.

In the present study, heat transfer measurements of a spherically sharp cone were conducted in three shock tunnels at LHD, which were responsible for providing the nonequilibrium (JF10) or perfect gas flows (JF8A and JF12), respectively. Different Reynolds numbers are also considered. The surface temperature is measured by using the E-type coaxial thermocouples or thin film gauges. And numerical analysis using the CFD technique has also been conducted. Through the assessment of data accuracy and consistency between each facility, we aim to establish practical guidelines for the complementary use of these ground-based test facilities and provide reliable database for CFD validation.

2 Experimental Setup

2.1 Facilities

The experimental program was conducted in the JF8A, JF10, and JF12 shock tunnels, which were reflected shock tunnels using high-pressure air or detonation driving technique. These facilities are common in the sense that they cover hypersonic speed regime, but there exist large differences regarding the flow properties and the tunnel specifications. JF8A is a middle-sized shock tunnel, and several times of experiments per day are possible. This is favorable as for data productivity, but the flow enthalpy is much lower and attainable. Reynolds number is much higher compared to the other two facilities. JF10 is a high-enthalpy shock tunnel which can provide high-temperature gas conditions for hypersonic flight, and real gas effect can also be studied. JF12 is the largest shock tunnel in the world with the nozzle exit diameter of 2.5 m, capable of replicating flight conditions for $\text{Ma}5\sim9$ at altitude of 25 ~ 50 km, and integrated vehicle/engine is possible to test. The major specifications of the three shock tunnels are shown in Table 1, and details can be seen in literature [4, 5]. Hence these facilities should be the compliments of each other, taking advantage of a merit of one facility and compensating a shortcoming of the others.

Table 1 Facility comparison

	JF8A	JF10	JF12
Operation mode	High-pressure air	Forward detonation	Backward detonation
Flow duration time	30 ms	5 ms	130 ms
Nozzle shape	Contoured	Conical	Contoured
Nozzle diameter	0.8 m	0.5 m	2.5 m
Maximum H_0	1.3 MJ/kg	20 MJ/kg	5 MJ/kg
Maximum Re	$4.2 \times 10^7/\text{m}$		$4 \times 10^6/\text{m}$

2.2 Sensors

Thin film resistance gauges, with a diameter of 2.2 mm, were installed in the JF8A test model due to their short rise times and high electrical output per degree rise in temperature. However, they are prone to thermal damage and rapid erosion by small particles in high-enthalpy flows of JF10 and JF12, and the lifetime of each gauge is limited to one or two shots. Thus, homemade E-type (chromel-constantan) coaxial thermocouples, 1.4 mm in diameter, were installed in these two shock tunnel models, which turned to have fast response times and can be flush-mounted. From the measured surface temperature T , the heat flux is calculated according to Schults and Jones [6] as follows:

$$\dot{q}(t_n) = 2\sqrt{\frac{\rho ck}{\pi}} \sum_{i=1}^n \frac{T(t_i) - T(t_{i-1})}{\sqrt{t_n - t_i} - \sqrt{t_n - t_{i-1}}} \quad (1)$$

where ρ , c , and k are the density, heat capacity, and heat conductivity of the sensor material and T and t are the temperature and time, respectively.

2.3 Models

A relatively simple model configuration was selected to alleviate uncertainties coming from the model geometry complexity. It was shown in Fig. 1 a 7 deg half-angle spherically sharp cone. Considering the nozzle exit diameter of the facilities, the model with an overall length of 590 mm was chosen for the JF10 shock tunnel and 1100 mm for the JF8A and JF12 shock tunnels.

2.4 Test Conditions

Reservoir pressure was measured using a piezoelectric pressure transducers mounted at the end of the shock tube. Other reservoir parameters were computed using the measured shock tube filling pressure, shock speed, and nozzle reservoir

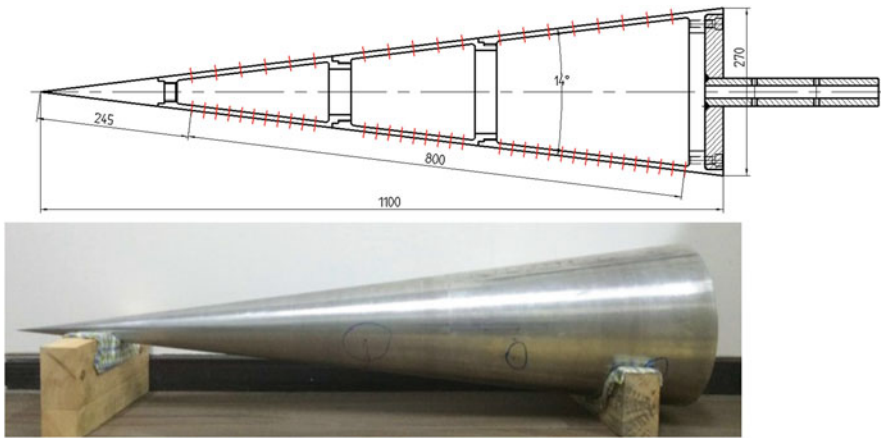


Fig. 1 Experimental models in JF8A

Table 2 Test conditions

	JF8A	JF10	JF12
P_0 (MPa)	1.2	13.5	2.2
H_0 (MJ/kg)	0.6	16	3.3
T_∞ (K)	67.5	435	293
ρ_∞ (kg/m ³)	2.7×10^{-2}	7.0×10^{-4}	5.0×10^{-3}
u_∞ (m/s)	1054	4979	2343
Re/L (/m)	6.4×10^6	1.5×10^5	6.5×10^5

pressure. Based on the reservoir conditions, the freestream was subsequently determined by numerical rebuilding of nozzle flow [7]. The accuracy of CFD analysis of the nozzle flow had also been judged by experiments taken in the freestream, such as static pressure, pitot pressure, and stagnation point heat flux. The reservoir and freestream conditions in our test were shown in Table 2. Subscript “0” represents the reservoir condition and “ ∞ ” for freestream condition. Reynolds number $Re = \frac{\rho_\infty u_\infty L}{\mu_\infty}$, with the characteristic length L , represents for model length. In addition, the experiments were conducted at the surface temperature of 290 K (room temperature). And the angle of attack was set to zero in all the experiments.

3 Numerical Method

As a valuable complement for the analysis of experimental results, such as boundary layer parameter determination, numerical simulations were used in the paper. And calculating heat transfer had also been compared with the experiments under laminar flows. The governing equations employed were the axisymmetric, compressible Navier-Stokes equations. Considering the test conditions of the three shock tunnels

and the computing cost, two sets of computation procedure were used in this paper. Calorically perfect gas was chosen for the JF8A and JF12 flow conditions, while thermal chemical nonequilibrium for the JF10 conditions. Beyond that, they were both based on the finite difference method of AUSMPW+ Scheme [8], and point implicit scheme of LU-SGS [9] was used. On the solid wall, the no-slip condition for velocity is considered, and the temperature is prescribed to the room temperature. The chemical composition on the body surface is considered either fully catalytic or non-catalytic to chemical reactions. The numerical heat flux is calculated by summing three contributing parts: translational temperature model flux, vibrational temperature model flux, and diffusion model flux as follows (only translational temperature model flux is considered for JF8A and JF12 condition):

$$q_w = k \frac{\partial T}{\partial n} + k_v \frac{\partial T_v}{\partial n} + \sum_{i=1}^{ns} h_i \rho D_i \frac{\partial c_i}{\partial n} \quad (2)$$

4 Results and Discussion

In the paper, the experimental results of the sharp cone in three different shock tunnels were explored and compared with each other. Since the sharp cone results in JF10 and JF12 could be found in the literature [10], we mainly focus on the results in JF8A and its comparison with the other two. The typical stagnation pressure and sensor curves were shown in Fig. 2, with an effective test time from 19 to 26 in the legend. Since the Reynolds number in JF8A was $6.4 \times 10^6/\text{m}$, transition and turbulent flow existed on the sharp cone surface, where it can also be distinguished by the different signal to noise ratio of the curves, whereas the other two shock tunnels were only laminar flow due to their much lower Reynolds number.

In order to be able to compare the results between different conditions, such as results from flight and ground tests or from different shock tunnel conditions, it is necessary to reduce the data to a suitable nondimensional form. Heat transfer rate is typically normalized into a Stanton number (St). It is known that heat transfer is the effect of boundary layer parameters to the wall, which would be affected by the freestream flows, such as shock strength or dissociation. Therefore, it is necessary to normalize the heat transfer using the boundary layer parameters rather than the freestream flows while trying to compare the experimental data from different ground facilities. Fortunately, the boundary layer parameters are easily to be obtained with the help of numerical simulation, but not for the heat flux which is relatively difficult with accurately calculation. St and Re_x are defined in Eq. (3). Subscript e represents for the boundary layer edge parameters and w for the wall parameters. r is the recovery factor, where $r = \sqrt{Pr}$ for laminar flows [11]. Pr is the Prandtl number, which is assumed to be constant, a fair approximation for most conditions of interest:

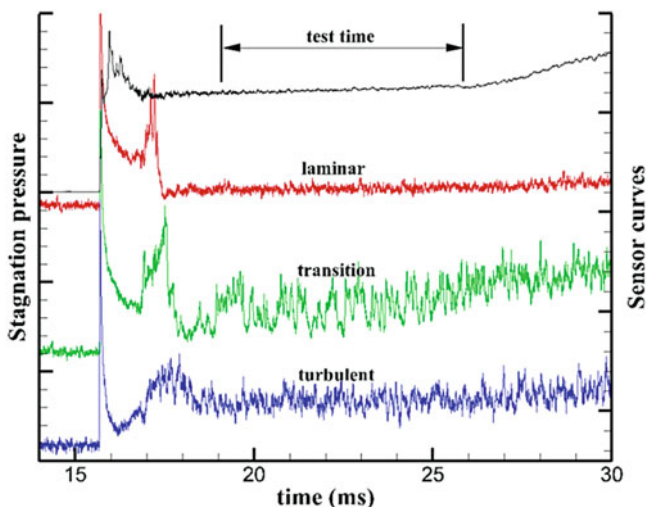


Fig. 2 Stagnation pressure and sensor curves in JF8A

$$St = \frac{q_w}{\rho_e u_e (H_0 - 0.5 \times u_e^2 (1 - r) - H_w)} \quad Re_x = \frac{\rho_e u_e x}{\mu_e} \quad (3)$$

In the previous literature [10], we developed a parameter, defined as the product of the Stanton number and the square root of the Reynolds number, which was found to be more characteristic for the aerodynamic heating phenomena encountered in hypersonic flight under laminar flows. This parameter can almost eliminate the variability caused by the different flow conditions, whether or not the flow is in dissociation or the boundary condition is catalytic. That was:

$$St = \frac{G \left(Ma_e, Pr, \gamma, T_w / T_e \right)}{\sqrt{Re_x}} = \frac{0.73}{\sqrt{Re_x}} \quad (4)$$

And Hornung [12] developed the similar relations for turbulent flows:

$$St = \frac{0.191}{Pr^{2/3} (\ln(0.046 Re_x))^2} \quad (5)$$

Gas condition under laminar flows for JF8A was a perfect gas, and heat transfer on a sharp cone can be obtained by solving boundary layer equations easily [11]. And the turbulent results were obtained using Eq. (5). Comparison between Exp and theory in Fig. 3 showed that the experiment was 10% smaller than the theoretical value. The reason was still in analysis. However, it was acceptable for heat transfer measurements in hypersonic flows.

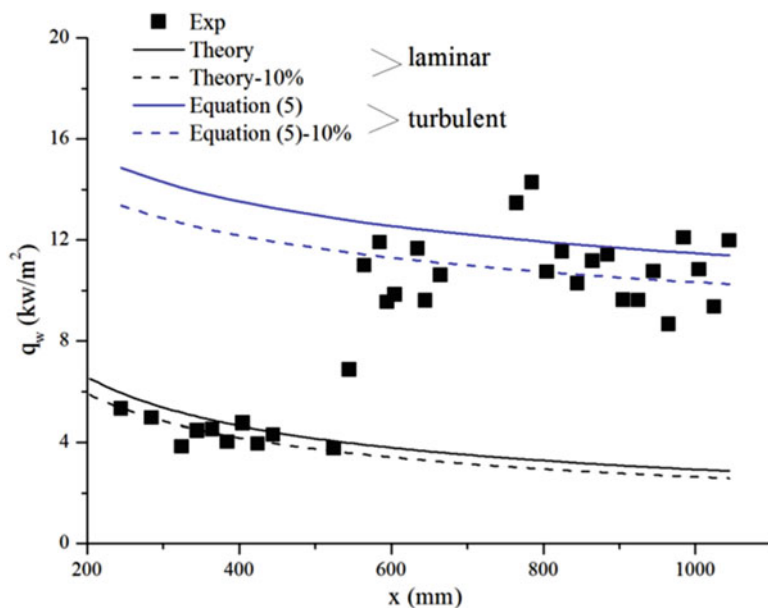


Fig. 3 Heat transfer data comparison between Exp and theory in JF8A

Figure 4 showed the Stanton number-Reynolds number relationship for the three shock tunnels, including experimental data, CFD, and a fitting line. And it needed to be emphasized that St and Re_x were defined using the boundary layer parameters in Eq. (4). Logarithmic coordinates were used to give an intuitive expression of constant A , which was 0.73 for laminar flows. It can be seen from Fig. 4 that although the Reynolds numbers were quite different from each other, the magnitude of 10^4 for JF10, 10^5 for JF12, and 10^6 for JF8A, the laminar heat transfer along the sharp cone showed the same regularity under parameter A , whether or not the flow is in dissociation. Flow chemistry of JF10 condition had small effect on it.

5 Conclusion

A comparative study had been conducted to investigate the hypersonic aerodynamic heating using a sharp cone model configuration between the three hypersonic facilities at LHD. From the experimental and numerical results obtained, the following conclusions were drawn. Parameter A , defined as the product of St and the square root of Re_x , was found to be a useful similarity parameter, where Stanton number-Reynolds number relationship shows almost the same regular in the three shock tunnel laminar conditions. It is noted that St and Re_x should be normalized using the boundary layer parameters. Work is presently underway to perform uncertainty analysis of the experimental data in JF8A shock tunnel and to extend the present study to higher Reynolds number flows.

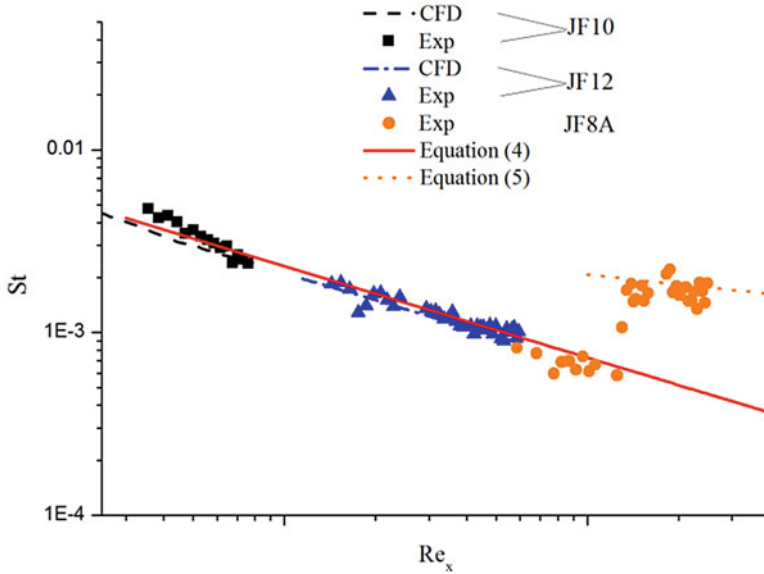


Fig. 4 Stanton number-Reynolds number relationships in the three shock tunnels

Acknowledgments This work was supported by the National Natural Science Foundation of China (Grant Nos. 11402275 and 11472280).

References

1. S.L. Gai et al., Stagnation point heat flux in hypersonic high enthalpy flows. *Shock Waves* **2**, 1 (1992)
2. T. Kishimoto et al., *High Enthalpy Flow Computation and Experiment Around the Simple Bodies* (Special Publication of National Aerospace Laboratory SP-29, Tokyo, 1996)
3. W.Z. Dong et al., Numerical analysis for correlation of standard model testing in high enthalpy shock facility and flight test. *Exp. Meas. Fluid. Mech.* **16**, 2 (2002)
4. Z. L. Jiang et al., Experiments and development of the long-test-duration hypervelocity detonation-driven shock tunnel (LHDst), AIAA 2014-1012
5. F.K. Lu et al., Advanced hypersonic test facilities, in *Progress in Astronautics and Aeronautics*, 2002
6. D.L. Schultz et al., Heat transfer measurements in short duration facilities, AGARD-AG-165, 1973
7. Q. Wang, *Experimental Study on Characteristics of Heat Transfer and Electron Density in High Enthalpy Flow* (Institute of Mechanics, Chinese Academy of Sciences, Beijing, 2013)
8. K.H. Kim et al., Methods for the accurate computations of hypersonic flows: I. AUSMPW+ scheme. *J. Comput. Phys.* **174**, 1 (2001)
9. A. Jameson et al., Lower-upper implicit schemes with multiple grids for the Euler equations. *AIAA J.* **25**(7) (1987)

10. Q. Wang et al., Comparative study on aerodynamic heating under perfect and nonequilibrium hypersonic flows. *Sci. China Phys. Mech.* **59**(2) (2016)
11. F.M. White, *Viscous Fluid Flow*, 2nd edn. (McGraw-Hill, New York, 1991)
12. P. Germain, et al., Transition on a sharp cone at high enthalpy: new measurements in the shock tunnel T5, AIAA 93-0343